

Article

Dynamic Windows with Neutral Color, High Contrast, and Excellent Durability Using Reversible Metal Electrodeposition



There is strong demand for dynamic windows, which reversibly darken upon application of a voltage, both for energy saving and aesthetic reasons. The use of metals, which are excellent attenuators of visible light, as the optically active material in dynamic windows is an intriguing, yet little explored approach due to the difficulty of reversibly and uniformly electrodepositing metals. We construct robust dynamic windows that possess neutral color, high contrast, and excellent durability based on the uniform reversible electrodeposition of metals.

Christopher J. Barile, Daniel J. Slotcavage, Jingye Hou, Michael T. Strand, Tyler S. Hernandez, Michael D. McGehee

mmcgehee@stanford.edu

HIGHLIGHTS

Robust dynamic windows based on reversible metal electrodeposition constructed

Tunable transparency with fast switching times and high optical contrast

Uniform metal electrodeposition over 25 cm² achieved using an inert seed layer

No detectable deterioration in uniformity or contrast after more than 5,000 cycles

Article

Dynamic Windows with Neutral Color, High Contrast, and Excellent Durability Using Reversible Metal Electrodeposition

Christopher J. Barile,¹ Daniel J. Slotcavage,¹ Jingye Hou,¹ Michael T. Strand,¹ Tyler S. Hernandez,² and Michael D. McGehee^{1,3,*}

SUMMARY

Dynamic windows, which switch between transparent and opaque states upon application of a voltage, have applications in buildings, automobiles, and switchable sunglasses. Here, we describe dynamic windows based on the reversible electrodeposition of Cu and a second metal on transparent indium tin oxide electrodes modified by Pt nanoparticles. Three-electrode cyclic voltammetry experiments reveal that the system possesses high Coulombic efficiency (99.9%), indicating that the metal electrodeposition and stripping processes are reversible. Two-electrode 25-cm² windows without bus bars uniformly switch between a transparent state (~80% transmission) and a color-neutral opaque state (<5% transmission) in less than 3 min. These devices switch at least 5,500 times without degradation of optical contrast, switching speed, or uniformity. Taken together, these results indicate that dynamic windows based on reversible metal electrodeposition are a promising alternative to those using traditional electrochromic materials.

INTRODUCTION

There is burgeoning interest in commercializing dynamic windows that enable electronic control of visible light and solar energy. Two companies recently raised more than \$600 million in private investments based on the potential of dynamic windows to increase occupant comfort and energy efficiency.^{1,2} In buildings, dynamic windows result in an average of 10% energy savings over static low-E windows due to reduced lighting, heating, and cooling costs.^{3,4} In addition, dynamic windows look substantially better than windows with blinds and are far more likely to be adjusted optimally since they can be automated with a computer and incorporated into smart homes and the Internet of Things. Dynamic windows can also be implemented in the sunroofs of vehicles and in switchable sunglasses, which would outperform those using passive photochromic glasses that darken upon exposure to UV light.

The properties of metals make them ideal light-modulating materials for dynamic windows. Due to their high extinction coefficients, metals are highly opaque at thicknesses of only tens of nanometers,⁵ which allows for the construction of windows with excellent optical contrast. Additionally many metals are chemically inert, photostable, and color neutral.⁶ Dynamic windows with metal as the optically active material utilize the reversible electrodeposition of a metal on a transparent conducting electrode. During window tinting, electrochemical reduction of a colorless cation of a metal salt in the electrolyte of the device to a solid thin film of elemental metal

Context & Scale

Controlling lighting and heating through the use of dynamic windows substantially decreases the energy consumption of buildings. Currently, dynamic windows are commercialized on only a small scale due to problems associated with durability, color, switching speed, and cost. Most dynamic windows utilize electrochromic materials, which change their transmission properties upon application of a voltage. The vast majority of research on dynamic windows over the past four decades has focused on transition metal oxides or polymeric materials as electrochromic materials. The use of metals, which are excellent attenuators of visible light, as the optically active material in dynamic windows is an intriguing, yet little explored alternative approach. In this work, we construct robust dynamic windows that possess neutral color, high contrast, and excellent durability based on the uniform reversible electrodeposition of metals.

occurs. Oxidation of metal hidden behind the frame of the window balances this reduction reaction. The net result is the reversible electrochemical movement of metal between the two electrodes of the device.

Despite the ideal properties of metals, dynamic windows based on reversible metal electrodeposition that simultaneously exhibit fast switching times, good durability, tunable transparency, and chemical stability have not yet been demonstrated. The difficulty of reversibly and uniformly electrodepositing metals on a transparent substrate over a large area is the key challenge hindering the development of metal-based dynamic windows. As a result, in lieu of metals, most dynamic windows use electrochromic materials such as transition metal oxides or polymers, which change their transmission characteristics upon application of a voltage.^{7,8} However, despite significant private funding and decades of academic research, electrochromic windows are not commercialized on a large scale due to problems associated with color, cost, durability, and switching speed.⁹

Other dynamic window technologies include polymer dispersed liquid crystals (PDLCs) and thermochromic windows.^{10,11} While an attractive feature of PDLCs is that they switch within milliseconds, they switch between a transparent state and a bright hazy state whereby light is scattered. This haze makes them unsuitable for any application in which maintaining a window view is important. Thermochromic windows, which switch in response to a temperature change, are also less than ideal due to a lack of user control.

Dynamic windows based on reversible metal electrodeposition are less explored than those using chromogenic materials or PDLCs. Devices only 1–4 cm² in area utilizing various Ag-based electrolytes have been the most investigated, but suffer from poor durability or Coulombic efficiency.^{12–14} The most promising transparent conducting electrodes for dynamic windows are glass surfaces coated with thin films of indium tin oxide (ITO) or fluorine-doped tin oxide (FTO) due to their high transparency, low sheet resistance, and low cost.¹⁵ However, the surface conductivities of ITO and FTO are not uniform due to heterogeneous surface chemistry.¹⁶ For this reason, the nucleation of metal electrodeposits on ITO or FTO surfaces is difficult to control and frequently results in nonuniform metal electrodeposition. Nonuniform deposition results in light and dark portions of the window during switching, yielding a window that is only optically uniform when there are enough metal electrodeposits across the entire electrode area to render all portions of the window completely opaque. Therefore, the problem of nonuniform deposition precludes the construction of a dynamic window that possesses tunable transparency. For example, reversible metal electrodeposition has been used to elicit binary tunability for display applications.^{17,18} In other words, each segment of the display could only switch between completely opaque and completely transparent without any intermediate control of transparency.

In this paper, we develop 25-cm² dynamic windows based on the reversible electrodeposition of Cu-Pb or Cu-Ag that switch uniformly between transparent (~80% transmission) and opaque states (<5% transmission) in less than 3 min. The devices consist of an ITO working electrode modified with Pt nanoparticles anchored via a self-assembled monolayer (SAM) of 3-mercaptopropionic acid and a metal counter-electrode frame. The Pt nanoparticles enable uniform electrodeposition by facilitating nucleation across the area of the ITO electrode. Metal electrodeposition occurs preferentially on the inert Pt seed layer, providing a stable platform for reversible metal electrodeposition over many cycles. This architecture enables us

¹Department of Materials Science and Engineering, Stanford University, Stanford, CA 94305, USA

²Department of Chemistry, Stanford University, Stanford, CA 94305, USA

³Lead Contact

*Correspondence: mmcgehee@stanford.edu
<http://dx.doi.org/10.1016/j.joule.2017.06.001>

to construct dynamic windows with a nontoxic gel electrolyte that cycle at least 5,500 times without degradation in uniformity or optical contrast.

RESULTS AND DISCUSSION

Electrolyte Selection for Electrodeposition

Electrolyte composition dramatically affects the uniformity and reversibility of metal electrodeposition.¹⁹ Water is an ideal solvent from which to reversibly electrodeposit metals due to its ability to dissolve many metal salts at high concentrations and to disassociate metal cations from their counter anions. Although reversible nonaqueous electrodeposition is feasible under certain conditions,²⁰ high-deposition overpotentials are common due to increased ion pairing in organic solvents, which frequently leads to undesirable side reactions. The temperature range of the solvent used in dynamic windows is an important consideration for practical device operation. While the 0°C–100°C range for water is acceptable for most building applications in which the interior temperature is controlled, this range is unsuitable for use in automotive glass. Even for elevated temperatures below the boiling point of water, a high electrolyte vapor pressure necessitates that the device is well sealed to prevent solvent loss. The range of aqueous electrolytes could be extended through the use of antifreeze or cross-linked gels. Due to their advantageous electrochemical properties, we chose to develop aqueous electrolytes as a starting point for dynamic windows utilizing reversible metal electrodeposition.

With water selected as a solvent, we next identified promising metals to electrodeposit. The selected metal ions must electrodeposit at a voltage more positive than that of H₂ production from water. Under standard conditions, the thermodynamic voltage of H₂ production from water versus the standard hydrogen electrode (SHE) varies with pH according to the equation: $E^\circ = -0.059 \text{ V} \times \text{pH}$. Less noble metals with more negative standard reduction potentials are more difficult to electrochemically reduce and thus electrolytes containing these metals are more likely to suffer from H₂ production as a side reaction, with the exact voltage limits determined by the solution pH and the overpotentials of the two competing reactions.

Another attribute that affects the utility of a metal electrodeposition system is the oxophilicity of the metal. More oxophilic metals have a greater propensity to form passivating metal oxides on the surface of the metal once they are electrodeposited, which leads to irreversibility. In addition, highly oxophilic metals more readily form insoluble hydroxides or oxides in solution under relatively basic conditions.

One important metric of dynamic windows is coloration efficiency, which is the electrode area that can be switched to a given optical contrast per unit of electrical charge passed. A higher coloration efficiency means the window can operate at a lower current density for a given switching speed. This lower current density results in less Ohmic drop across the electrodes, which is advantageous for maintaining metal electrodeposit uniformity. Given the extinction coefficient, oxidation state, and molar volume of a metal, the coloration efficiency of a metal electrodeposition system can be computed using the Beer-Lambert relationship.²¹ Table 1 lists the theoretical coloration efficiencies for different metals at 600 nm assuming a completely uniform film and a contrast ratio of 60%.

Considering the oxophilicity, coloration efficiency, reduction potential, and cost of different metals in Table 1, Pb is a promising metal for reversible electrodeposition given its high theoretical coloration efficiency and low oxophilicity. Since Pb is one of the most ineffective catalysts for H₂ production,²⁴ an electrolyte for Pb

Table 1. Properties of Some Metals Relevant to Dynamic Windows Based on Reversible Metal Electrodeposition

Metal	Most Common Oxidation State	Oxophilicity	Theoretical Coloration Efficiency (cm ² /C)	Standard Reduction Potential (V versus SHE)	Cost (\$/kg)
Au	1	0.0	101	1.83	40,420
Pt	2	0.1	62	1.19	31,590
Pd	2	0.0	52	0.92	25,980
Ag	1	0.2	101	0.80	590
Cu	2	0.2	42	0.34	6
Bi	3	0.2	77	0.31	9
Pb	2	0.1	132	-0.13	2
Sn	2	0.4	122	-0.13	20
Ni	2	0.2	46	-0.25	10
Co	2	0.4	42	-0.28	54
In	3	0.4	62	-0.34	230
Cd	2	0.2	80	-0.40	1
Fe	2	0.4	57	-0.44	0.3
Ta	3	0.8	46	-0.60	124
Cr	3	0.6	19	-0.74	7
Zn	2	0.2	59	-0.76	3

Standard reduction potentials listed are for the unligated metal ions to elemental metal. Costs are bulk US market prices as of March 28, 2017. Oxophilicity values are taken from literature.²² Coloration efficiencies are calculated using a method proposed previously assuming no reflection.²³

electrodeposition will have a much wider voltage range than its standard potential suggests. An additional benefit of Pb is that reversible electrodeposition systems are already well explored in the context of Pb-acid batteries.²⁵ We therefore selected Pb as a proof-of-concept electrodeposition system for dynamic windows. Table 1 indicates that Ag also has promising electrochemical properties, so we developed devices with this metal as a nontoxic alternative to Pb. For both systems, we coelectrodeposited Cu. In the presence of Cl⁻ and other additives, Cu improves the uniformity of codeposited metals through a mechanism mediated by Cu(I).²⁶ Although electrodeposition of pure Cu can be conducted with good uniformity, the red color of Cu is undesirable for window applications, and hence we electrodeposit Cu and a second metal in this work.

Cu-Pb Electrolyte

The Cu-Pb electrolyte we developed consists of Pb(ClO₄)₂, CuCl₂, Cu(ClO₄)₂, and LiClO₄. Pb(ClO₄)₂ serves as a source of Pb²⁺ charge balanced by the non-coordinating ClO₄⁻ anion. The electrolyte contains both CuCl₂ and Cu(ClO₄)₂ as sources of Cu²⁺. The CuCl₂ serves as a source of Cl⁻, which is known to be a Cu electrodeposition and stripping accelerant.^{27,28} However, the low solubility of PbCl₂ reduces the concentration of Cl⁻ in solutions containing Pb²⁺. For this reason we added Cu(ClO₄)₂ to the electrolyte which, as an additional source of Cu²⁺, shifts the speciation of Cl⁻ in the electrolyte to favor the formation of soluble Cu-Cl complexes such as CuCl₄²⁻ due to Le Châtelier's principle. Finally, we added a high concentration of LiClO₄ as a supporting electrolyte to increase the ionic conductivity of the solution.

Figure 1 shows the transmission of a Pt-modified ITO-on-glass electrode inside a spectroelectrochemical cell containing the Cu-Pb electrolyte as it is electrochemically

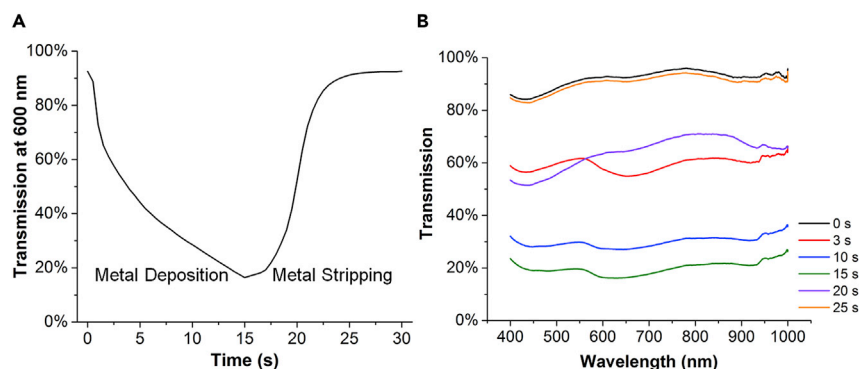


Figure 1. Transmission during Metal Electrodeposition and Stripping

(A) Transmission at 600 nm of a Pt-modified ITO-on-glass electrode in a spectroelectrochemical cell containing 100 mM $\text{Pb}(\text{ClO}_4)_2$, 50 mM CuCl_2 , 50 mM $\text{Cu}(\text{ClO}_4)_2$, and 1 M LiClO_4 in H_2O as a function of time. The electrode is polarized at -0.55 V versus Ag/AgCl for the first 15 s and then switched to $+0.65$ V for the remaining 15 s.

(B) Transmission of this electrode as a function of wavelength after 0 s (black), 3 s (red), 10 s (blue), 15 s (green), 20 s (purple), and 25 s (orange).

See also Figures S1–S3.

switched. The initial transmission of the electrode at 600 nm is 92% due to absorption of visible light by the ITO-on-glass electrode. Polarizing the electrode to -0.55 V versus Ag/AgCl results in cathodic current due to Cu and Pb electrodeposition, which reduces the transmission of the electrode to 18% after 15 s (see Figures 1A and S1). Auger electron spectroscopy reveals that Pt, In, Sn, and O are present on the Pt-modified ITO electrode as expected and that the metal thin film contains 85% Cu and 15% Pb when electrodeposited at -0.35 V (see Figure S2). Alternatively, increasing the deposition time to 40 s allows for additional metal deposition to occur, causing the transmission of the electrode to decrease to 1%–2% from 400 to 2,500 nm (see Figure S3). This result demonstrates that the electrodeposited metal can be made highly opaque to both visible and infrared light, giving an electrode contrast ratio of $\sim 90\%$.

After metal deposition, we switched the voltage of the electrode to $+0.65$ V to oxidize Cu and Pb to Cu^{2+} and Pb^{2+} . The dissolution of the metal electrodeposits causes the transmission of the cell to return to its original 92% value within an additional 15 s (see Figure 1A). Importantly, the spectral response of the electrode remains relatively flat across all wavelengths measured during the switching process (see Figure 1B), resulting in a color-neutral opaque state.

Evaluation of Cycle Life

We next evaluated the cyclability of the Cu-Pb reversible electrodeposition system. Figure 2A displays the maximum and minimum transmission values at 600 nm of a Pt-modified electrode as it switches between transparent and opaque states. Each cycle consists of applying a potential of -0.35 V for 60 s to induce metal deposition followed by $+0.45$ V for 60 s to elicit metal dissolution (see Figure S4). For the Pt-modified electrode, the contrast ratio remains around 50% over the course of 1,000 cycles. By increasing the deposition voltage to -0.55 V and depositing for only 15 s, we maintain reversible electrodeposition with a contrast ratio greater than 60% over the 4,000 cycles tested (see Figure S5). At an even higher deposition voltage of -0.75 V and a correspondingly smaller deposition time of 10 s, the electrode initially exhibits a high contrast ratio of $\sim 90\%$. However, this contrast ratio

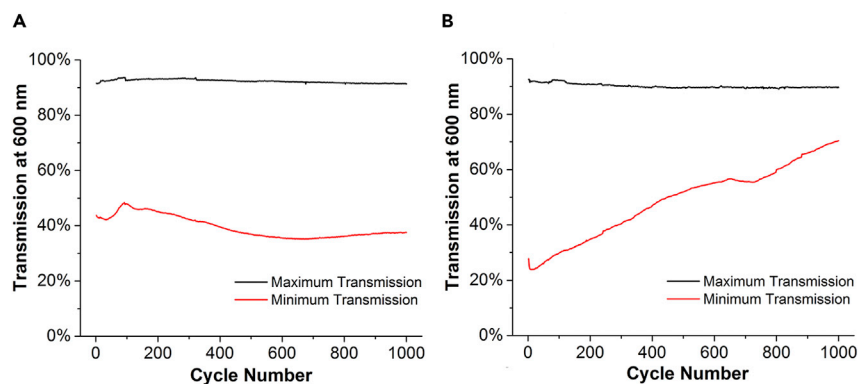


Figure 2. Maximum and Minimum Transmission at 600 nm during Electrode Cycling

(A and B) Maximum (black) and minimum (red) transmission at 600 nm of the Cu-Pb electrodeposition system as a function of cycle number with a Pt-modified (A) and unmodified (B) ITO-on-glass electrode. For each cycle, the electrode was held at -0.35 V for 60 s to elicit metal deposition followed by $+0.45$ V for 60 s to induce metal stripping. See also [Figures S4–S6](#).

steadily decreases over 1,000 cycles (see [Figure S6](#)). Rapid nonuniform electrodeposition occurs at this high voltage, resulting in rough porous deposits, which are difficult to electrochemically dissolve during the subsequent stripping steps.²⁹ These results demonstrate that although increasing the magnitude of the deposition voltage decreases the switching speed of the electrode, the reversibility of the system cannot be maintained at higher deposition voltages. More importantly, with properly selected voltages reversible metal electrodeposition can be sustained for at least several thousands of cycles.

In contrast to a Pt-modified electrode switched using a deposition voltage of -0.35 V, an electrode without Pt exhibits poor cyclability using the same deposition voltage. The minimum transmission of an electrode without Pt increases steadily to $\sim 70\%$ after 1,000 cycles, which corresponds to a contrast ratio of only 20% (see [Figure 2B](#)). Therefore, the presence of a Pt layer on the electrode significantly enhances the durability of the electrodeposition system.

Morphology of Metal Electrodeposits

To probe why a Pt layer increases the durability of the Cu-Pb electrodeposition system, we interrogated the morphology of the Cu-Pb electrodeposit as the electrodes cycle using scanning electron microscopy (EM). During the first cycle of metal electrodeposition on a Pt-modified electrode, dense platelet-like structures of Cu-Pb grow on the electrode surface (see [Figure 3A](#)). The morphology of the electrodeposit remains relatively consistent after 1,000 cycles (see [Figure 3B](#)), indicating that the electrodeposition and stripping processes are reversible. Cyclic voltammetry (CV) measurements using Pt-modified and unmodified ITO-on-glass electrodes demonstrate that Cu and Pb nucleation occurs more readily on Pt than on ITO (see [Figure S7](#)), indicating that the Pt serves as a seed for metal nucleation. On an electrode without a Pt seed layer, a low density of sphere-like Cu-Pb particles grow on the electrode during the first cycle of deposition (see [Figure 3C](#)). As the electrode switches over 1,000 cycles, these spheres break up into increasingly smaller particles with dramatically altered morphology (see [Figure 3D](#)). Taken together, these results demonstrate that the uniform distribution of stable nucleation sites imparted by the Pt layer enables reversible electrodeposition with consistent morphology.

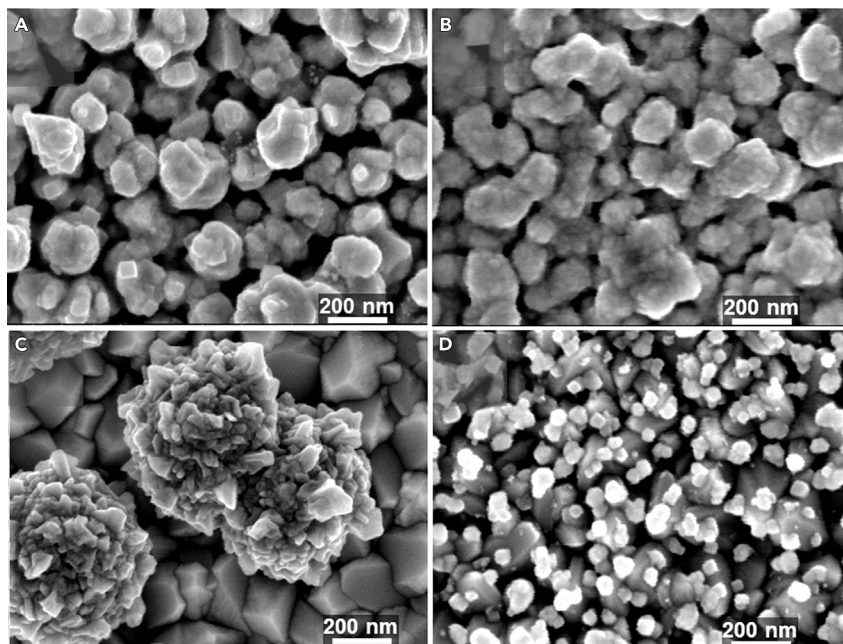


Figure 3. Scanning Electron Microscopy of Electrodeposits

(A–D) Scanning EM images after 30 s of metal deposition at -0.55 V on a Pt-modified electrode after 1 (A) and 1,000 (B) cycles of switching and on an unmodified ITO-on-glass electrode after 1 (C) and 1,000 (D) cycles of switching. Scale bars, 200 nm. See also [Figures S7–S9](#).

Coulombic Efficiency

Although the change in transmission during switching of the Cu-Pb system is 100% reversible, the calculated Coulombic efficiency for a CV of the solution (see [Figure S8](#)) is 90%, indicating that one or more side reactions occur. Two common side reactions in aqueous metal electrodeposition systems are the electrocatalytic reduction of H^+ to H_2 and the chemical oxidation of metal to metal oxides by O_2 .³⁰ The formal potential for the H_2 evolution reaction at the pH of the Cu-Pb electrolyte (-0.48 V versus Ag/AgCl at pH 4.5) is more negative than the range scanned in the CV experiment, indicating that this reaction is thermodynamically impossible under these conditions. To test whether oxidation of the metallic film by O_2 occurs, we performed CV of the Cu-Pb system under N_2 atmosphere (see [Figure S9](#)). Under N_2 the calculated Coulombic efficiency for the electrodeposition and stripping processes is 99.9%, indicating that the oxidation of the Cu-Pb film by O_2 to metal oxides is the primary side reaction that takes place when the voltammetry is performed in air. These metal oxides can then react with Cl^- in the electrolyte to form oxychloride species, which can dissolve back into the electrolyte.^{31,32} As a result, the transmission of the electrode is completely reversible even though the Coulombic efficiency is not 100% when the electrode is switched in air.

Two-Electrode 25-cm² Dynamic Windows Using a Nontoxic Cu-Ag Electrolyte

Having established a promising Cu-Pb electrodeposition system in a three-electrode cell on a small scale (3 cm²), we next developed practical 25-cm² two-electrode dynamic windows using a Cu-Pb gel electrolyte (see [Figure S10](#)). These devices consist of an ITO working electrode modified with Pt nanoparticles and a Cu metal counter-electrode frame with a glass backside (see [Figure 4A](#)). We subsequently substituted the Pb-containing electrolyte for one containing nontoxic Ag. This water-based electrolyte contains hydroxyethylcellulose to increase solution

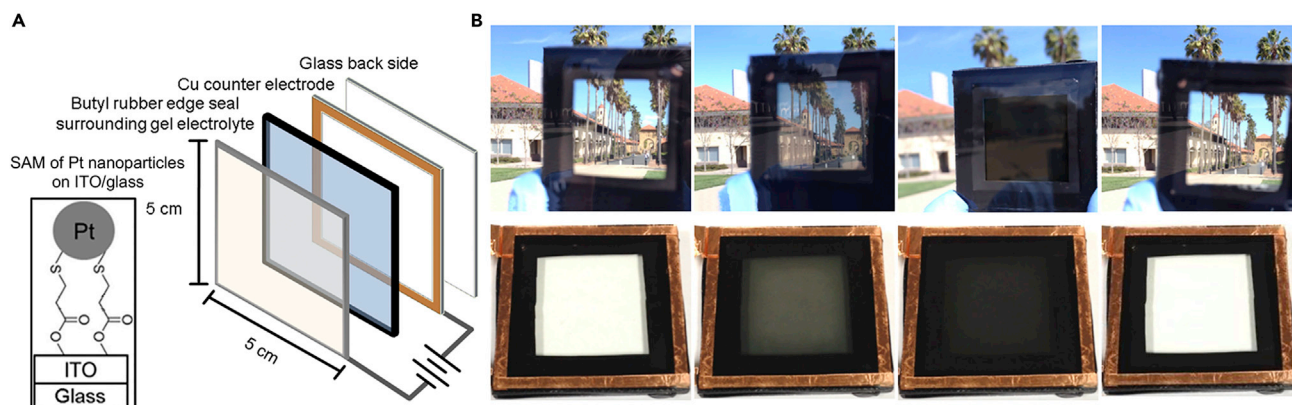


Figure 4. Schematic and Photographs of a 25-cm² Dynamic Window

(A) Schematic of a 25-cm² two-electrode dynamic window containing a Cu-Ag gel electrolyte with an ITO-on-glass working electrode modified with an SAM of Pt nanoparticles (inset).

(B) Photographs of the dynamic window during switching outside (top) and inside with a white background (bottom) after 0 s, 15 s, and 30 s of metal electrodeposition at -0.6 V and subsequently 30 s of metal stripping at $+0.8$ V (from left to right). See also [Figure S10](#).

viscosity, $\text{Cu}(\text{ClO}_4)_2$, $\text{Ag}(\text{ClO}_4)_2$, and a large concentration of LiCl to favor the formation of the soluble AgCl_2^- complex.

Using this electrolyte and device architecture, we constructed robust and color-neutral 25-cm² dynamic windows (see [Figure 4B](#)). Upon application of -0.6 V, metal deposition on the working electrode causes the initial 81% transmission of the device at 600 nm to decrease to $<20\%$ after 30 s and to $<5\%$ after 180 s (see [Figures 5A](#) and [5B](#)). Switching the voltage of the window to $+0.8$ V restores the original transparency of the device within ~ 70 s. We also tested the long-term stability of the transparent and opaque states of the dynamic window. In its opaque state, the transparency of the window fluctuates less than 1% over 24 hr when a small current is applied to oppose self-discharge (see [Figure 5C](#)). Since only a negligible amount of power is required to keep the window opaque over 24 hr (~ 130 nW/cm²) and no energy is consumed to keep the window transparent, significant power (~ 350 $\mu\text{W}/\text{cm}^2$) is only needed when switching the device (see [Figure S11](#)). The long-term durability of the dynamic window is also excellent. The contrast ratio elicited by 20 s of metal electrodeposition stays relatively constant, ranging from 47% to 53% for the duration of the 5,500 cycles tested (see [Figures 5D](#) and [S12](#)). Importantly, the transmission profile across the 25-cm² working electrode remains uniform throughout the 5,500 cycles (see [Figures S13–S15](#)), allowing the window to be stopped at any desired intermediate state at any point during cycling.

Optical Properties

The transmission of a dynamic window utilizing reversible metal electrodeposition as it cycles is intimately related to the morphology of the growing metal. For a completely uniform compact metal film, the Beer-Lambert law indicates that the transmission of an electrode will exponentially decrease with respect to the thickness of metal electrodeposited.²¹ From the amount of current passed during Cu-Pb electrodeposition (see [Figure S16](#)), the average thickness of metal electrodeposited as a function of deposition time can be inferred, assuming a completely uniform layer forms. The expected transmission of the electrode can then be calculated through a simple application of the Beer-Lambert law. This “uniform” model (see [Figure 6C](#), red) drastically overestimates the actual opacity of the device as it

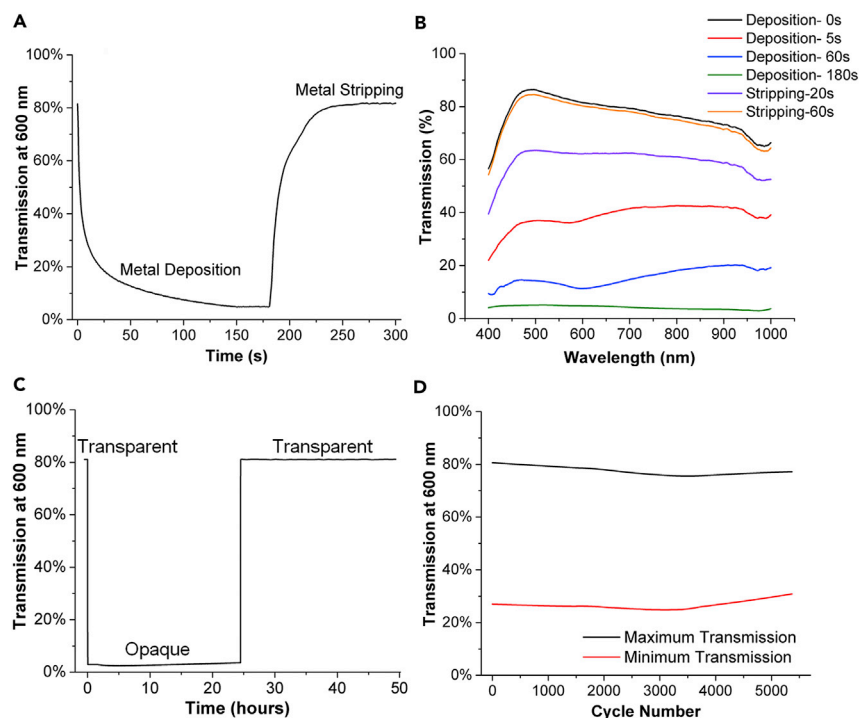


Figure 5. Transmission Profiles of a 25-cm² Dynamic Window

(A) Transmission of a 25-cm² dynamic window with a Cu-Ag gel electrolyte during metal deposition at -0.6 V and stripping at $+0.8$ V.

(B) Transmission of the same device as a function of wavelength after 0 s (black), 5 s (red), 60 s (blue), and 180 s (green) of metal deposition followed by stripping for an additional 20 s (purple) and 60 s (orange).

(C and D) Bistability test (C) and cycle test (D) of the windows.

See also [Figures S11–S15](#).

switches (black). This discrepancy arises because the morphology of the electrodeposited metal is not uniform and instead consists of “pillars.” As each pillar grows, it affects the overall transmission of the device less.

To account for the nonuniform morphology of the metal, we used atomic force microscopy (AFM) to map the height of the metal electrodeposits. The AFM results reveal the same platelet-like morphology found using scanning EM (see [Figure S17](#)). By recording AFM images as a function of electrodeposition time (see [Figures 6A and S18](#)), the growth of the metal deposits can be tracked in three dimensions. We transformed each pixel of the AFM images to a Beer-Lambert transmission value based upon the pixel’s height. The result is an exponential inversion of the AFM image (see [Figure 6B](#)). The overall transmission of the electrode is then modeled by calculating the average transmission across the entire area of the AFM image. The blue points in [Figure 6C](#) show that the resulting model accurately predicts the transmission of the electrode after 6, 12, and 30 s of electrodeposition. However, the modeling result deviates from the measured electrode transmission after 2 s of electrodeposition. In this case, the electrodeposit consists of many small (100–200 nm) unconnected metal particles, which give rise to plasmonic effects not accounted for in the model. Nonetheless, the model demonstrates that the transmission of the electrode does not follow a simple application of the Beer-Lambert law and can only be accurately predicted by accounting for the morphology of the metal deposits. Moreover, the more gradual change in

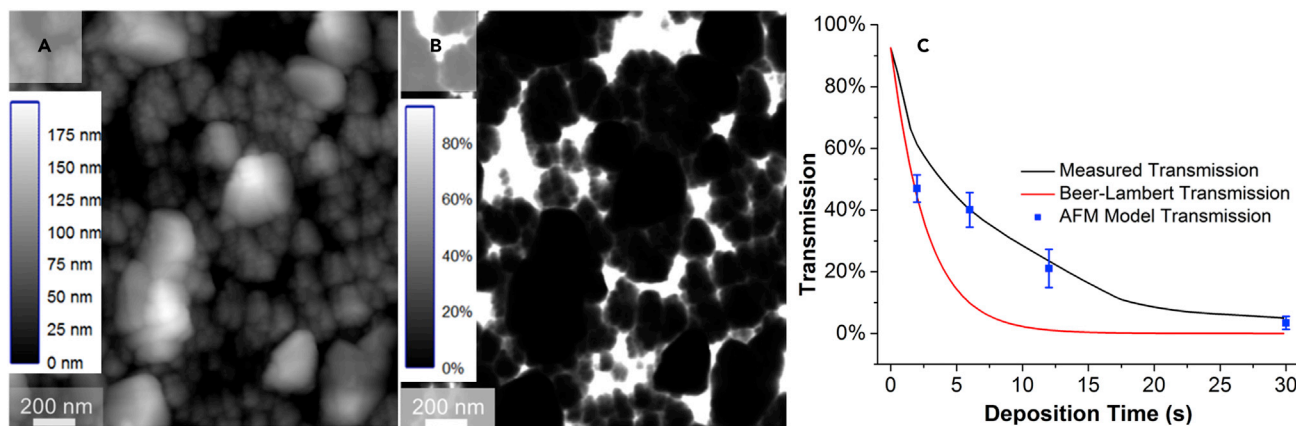


Figure 6. Analysis of Electrodeposit Morphology Using Atomic Force Microscopy

(A and B) AFM images of Cu-Pb electrodeposit formed after 12 s of electrodeposition at -0.55 V on a Pt-modified ITO-on-glass electrode (A) and the same surface wherein each pixel has been converted to a transmission value using the Beer-Lambert law (B).

(C) Transmission at 600 nm as a function of time during electrodeposition (black). The transmission curve is modeled using the Beer-Lambert law assuming uniform metal growth (red) and by accounting for the morphology measured by AFM (blue).

See also [Figures S16–S22](#).

transmission observed with respect to deposition time renders it easier to obtain spatially uniform transmission.

Measurement of the transmission and reflectance in an integrating sphere (see [Figure S19](#)) indicates that when the dynamic window is opaque ($<5\%$ transmission), only $\sim 20\%$ of visible light is reflected while the remaining $\sim 75\%$ of light is absorbed. At first glance, this behavior appears anomalous for metal films. For optically smooth metal films, a majority of incident light in the visible and infrared ranges is specularly reflected. However, the electrodeposition process discussed in this work does not form smooth metal films. Rather, electrodeposition forms aggregates of poorly connected metal particles with dimensions on the order of the wavelength of visible light (see [Figures S20 and S21](#)). Mie theory suggests that particles of this size will not primarily backscatter specularly as would a bulk metal film, but will instead scatter in many directions.³³ Multiple scattering events from the many particles that compose these electrodeposited metals significantly increase absorption probability, yielding the highly absorptive behavior observed from integrating sphere measurements.

Comparison with Electrochromic Materials

The majority of commercial dynamic windows utilize transition metal oxides, the most common of which is WO_3 . We suggest that the reversible metal electrodeposition systems reported in this work represent a competitive alternative. Whereas WO_3 switches between colorless and blue,³⁴ metals can be color neutral. Both the metal windows developed here and those using WO_3 have minute-order switching times and several-thousand-cycle lifetimes. The dynamic windows we constructed have a color efficiency of $\sim 90 \text{ cm}^2/\text{C}$ (see [Figure S22](#)) at a contrast ratio of 60%, which is comparable with the color efficiencies of those using WO_3 . Future improvements in the contrast ratio could be made through the use of electrodeposition leveling agents or modified seed layers that increase the uniformity of the metal film. Moreover, we anticipate that dynamic windows harnessing reversible metal deposition will be substantially cheaper than those using transition metal oxides. Metal oxide electrochromics are typically constructed by sputtering active layers hundreds of

nanometers or microns thick on both electrodes of the windows, a process which is expensive on the large scales needed.³⁵ In contrast, the optically dynamic components of the windows developed here are entirely solution processed. Additionally, whereas electrochromic windows must contain two transparent conducting electrodes, the dynamic windows presented in this work utilize only one transparent conducting electrode, which should further decrease materials and fabrication costs. Since only nanometers of Pt and Ag are used in these devices, the cost of these metals in the windows will not be significant. For example, a 1-ft² window with a 50-nm-thick layer of Ag and a 3-nm-thick layer of Pt would contain less than \$0.20 worth of Pt and less than \$0.03 worth of Ag. For all of these reasons, dynamic windows based on reversible metal deposition represent a promising alternative to electrochromic windows that merits further research and development.

EXPERIMENTAL PROCEDURES

Chemicals were received from commercial sources and used without further purification. Electrochemical studies were carried out using a CH Instruments 600 D Electrochemical Workstation (Austin, TX) or an SP-150 Biologic potentiostat. For experiments utilizing three electrodes, electrochemical potentials were measured and reported with respect to a “no-leak” Ag/AgCl (3 M KCl) reference electrode (eDAQ). Electrodes consisting of ITO-on-glass (Xinyan Technology, nominally 15 Ω /sq for 25 cm², nominally 10 Ω /sq for 3 cm²) were cleaned by successively sonicating in de-ionized H₂O with 5% Extran solution for 15 min, acetone for 15 min, and isopropanol for 15 min. The electrodes were subsequently dried under a stream of N₂.

Dynamic windows were constructed in either three-electrode or two-electrode configurations. Three-electrode devices utilized an ITO-on-glass or Pt-modified ITO-on-glass working electrode, Pt wire counter electrode, and Ag/AgCl reference electrode. The immersed geometric surface area of the working electrode was 3.0 cm², and electrochemical cells were assembled in a 4.5 × 2.0 × 1.0-cm glass cuvette (G205, CuvetteShop.com). Cu foil served as both the counter and reference electrodes in the two-electrode devices. The aqueous liquid Cu-Pb electrolyte consisted of 100 mM Pb(ClO₄)₂, 10 mM Cu(ClO₄)₂, 10 mM CuCl₂, and 1 M LiClO₄ and was used for experiments when the deposition voltage was −0.35 V. A more concentrated electrolyte containing 1 M LiClO₄, 100 mM Pb(ClO₄)₂, 50 mM Cu(ClO₄)₂, and 50 mM CuCl₂ was used when more negative deposition voltages were explored. All Cu-Pb electrolytes were cycled 100 times between +0.45 V and −0.55 V at a scan rate of 5 mV/in a three-electrode cell before use. The Cu-Pb gel electrolyte contained 3.3% hydroxyethylcellulose by weight.

Two-electrode experiments utilized 25 cm² Pt-modified or unmodified ITO-on-glass working electrodes and a Cu-Ag gel electrolyte. To make the Cu-Ag electrolyte, we prepared a solution nominally containing 10 mM AgClO₄, 15 mM Cu(ClO₄)₂, and 1 M LiCl in H₂O. After filtering away insoluble solids, a gel was formed by agitating a suspension containing the Cu-Ag liquid electrolyte and 3.3% hydroxyethylcellulose by weight. Either butyl rubber sealant or an ethylene-propylene-diene monomer rubber O-ring separated the two device electrodes.

Pt nanoparticles used to modify the working electrodes had average diameters of 3 nm and were purchased from Sigma-Aldrich. For working electrodes modified with an SAM of Pt nanoparticles, ITO-coated glass substrates were immersed in an ethanolic solution of 10 mM 3-mercaptopropionic acid for 24 hr. The substrates

were subsequently rinsed with ethanol and water before immersing them for 72 hr in a Pt nanoparticle solution that was diluted 1:3 with H₂O. After Pt immersion, the substrates were rinsed with water, dried with an N₂ gun, and used immediately in device construction. Cu tape was used to make electrical contact to the working electrode.

Transmission spectra recorded were measured with an Ocean Optics USB2000 spectrometer coupled with an Ocean Optics halogen light source (HL-2000-FHSA). Scanning EM images were obtained using an FEI XL30 Sirion microscope operated at an accelerating voltage of 5 kV. Auger electron spectroscopy was performed using a PHI 700 Scanning Auger Nanoprobe using a 10 kV/10 nA beam voltage/current. AFM images were recorded using a Park Systems XE-70 instrument. Optical images were taken with a Casio EXILIM Pro EX-F1 Compact Digital Camera. To quantify uniformity, we obtained grayscale photographs during switching, with the only source of illumination coming from a uniform light source behind each window. Reflection measurements were measured using a Jasco Model V670 UV-Vis-NIR spectrometer equipped with a 60-mm integrating sphere.

SUPPLEMENTAL INFORMATION

Supplemental Information includes 22 figures and can be found with this article online at <http://dx.doi.org/10.1016/j.joule.2017.06.001>.

AUTHOR CONTRIBUTIONS

C.J.B., D.J.S., and M.D.M. designed the experiments and analyzed the data. C.J.B., D.J.S., J.H., M.T.S., and T.S.H. performed the experiments. C.J.B. and M.D.M. wrote the paper. All authors discussed the results and commented on the manuscript.

ACKNOWLEDGMENTS

This research was funded by the Precourt Institute for Energy at Stanford. Part of this work was performed at the Stanford Nano Shared Facilities (SNSF). We thank L. Postak (Quanex) for Solargain® edge tape. D.J.S. and M.T.S. acknowledge the financial support of Stanford Graduate Fellowships. T.S.H. acknowledges a National Science Foundation Graduate Research Fellowship (No. NSF DGE-1656518).

Received: May 3, 2017

Revised: May 31, 2017

Accepted: June 14, 2017

Published: August 9, 2017

REFERENCES

1. Wesoff, E. (2015). View has raised more than \$500 million for smart adaptive windows. <https://www.greentechmedia.com/articles/read/View-Has-Raised-More-Than-500-Million-for-Smart-Adaptive-Windows>.
2. Stangel, L. (2017). South S.F. startup raises \$65M for its smart glass-tinting technology. <http://www.bizjournals.com/sanjose/news/2017/01/31/south-s-f-startup-raises-65m-for-its-smart-glass.html>.
3. Lee, S.E., Yazdani, M., and Selkowitz, S.E. (2004). The Energy-Savings Potential of Electrochromic Windows in the US Commercial Buildings Sector (Lawrence Berkeley National Laboratory), LBNL-54966.
4. View Glass. (2017). Energy benefits of View Dynamic Glass in workplaces. <http://viewglass.com/assets/pdfs/workplace-white-paper.pdf>.
5. Heavens, S.O. (1965). *Optical Properties of Thin Solid Films* (Dover Publications).
6. Callister, W.D., and Rethwisch, D.G. (2009). *Materials Science and Engineering: An Introduction*, Eighth Edition (John Wiley).
7. Mortimer, R.J. (2011). Electrochromic materials. *Annu. Rev. Mater. Res.* 41, 241–268.
8. Barile, C.J., Slotcavage, D.J., and McGehee, M.D. (2016). Polymer-nanoparticle electrochromic materials that selectively modulate visible and near-infrared light. *Chem. Mater.* 28, 1439–1445.
9. Runnerstrom, E.L., Llordes, A., Lounis, S.D., and Milliron, D.J. (2014). Nanostructured electrochromic smart windows: traditional materials and nir-selective plasmonic nanocrystals. *Chem. Commun.* 50, 10555–10572.
10. Murray, J., Ma, D., and Munday, J.N. (2017). Electrically controllable light trapping for self-powered switchable solar windows. *ACS Nano* 4, 1–7.
11. Kim, H., Kim, Y., Kim, K.S., Jeong, H.Y., Jang, A., Han, S.H., Yoon, D.H., Suh, K.S., Shin, H.S., Kim, T., and Yang, W.S. (2013). Flexible thermochromic window based on hybridized VO₂/Graphene. *ACS Nano* 7, 5769–5776.

- Araki, S., Nakamura, K., Kobayashi, K., Tsuboi, A., and Kobayashi, N. (2012). Electrochromic materials: electrochemical optical-modulation device with reversible transformation between transparent, mirror, and black. *Adv. Mater.* **24**, OP122–OP126.
- Laik, B., Carriere, D., and Tarascon, J. (2001). Reversible electrochromic system based on aqueous solution containing silver. *Electrochim. Acta* **46**, 2203–2209.
- Camilibel, I., Singh, S., Stocker, H.J., VanUitert, L.G., and Zydik, G.J. (1978). An experimental display structure based on reversible electrodeposition. *Appl. Phys. Lett.* **33**, 793.
- Ellmer, K. (2012). Past achievements and future challenges in the development of optically transparent electrodes. *Nat. Photon.* **6**, 809–817.
- Armstrong, N.R., Veneman, P.A., Ratcliff, E., Placencia, D., and Brumbach, M. (2009). Oxide contacts in organic photovoltaics: characterization and control of near-surface composition in indium-tin oxide (ITO) electrodes. *Acc. Chem. Res.* **42**, 1748–1757.
- Ziegler, J.P., and Howard, B.M. (1995). Applications of reversible electrodeposition electrochromic devices. *Sol. Energ. Mat. Sol. C* **39**, 317–331.
- Ziegler, J.P. (1999). Status of reversible electrodeposition electrochromic devices. *Sol. Energ. Mat. Sol. C* **56**, 477–493.
- Schlesinger, M., and Paunovic, M. (2010). *Modern Electroplating*, Fifth Edition (John Wiley).
- Aurbach, D. (1999). *Nonaqueous Electrochemistry* (CRC Press).
- Mayerhofer, T.G., Mutschke, H., and Popp, J. (2016). Employing theories far beyond their limits—the case of the (Boguer-) Beer-Lambert law. *Chem. Phys. Chem.* **17**, 1948–1955.
- Kepp, K.P. (2016). A quantitative scale of oxophilicity and thiophilicity. *Inorg. Chem.* **55**, 9461–9470.
- Zaromb, S. (1962). Theory and design principles of the reversible electroplating light modulator. *J. Electrochem. Soc.* **109**, 903–912.
- Quaino, P., Juarez, F., Santos, E., and Schmickler, W. (2014). Volcano plots in hydrogen electrocatalysis—uses and abuses. *Bellstein J. Nanotechnol.* **5**, 846–854.
- Pavlov, D. (2011). *Lead-Acid Batteries: Science and Technology* (Elsevier).
- de Oliveira, S.C., de Moraes, L.C., da Silva Curvelo, A.A., and Torresi, R.M. (2003). An organic aqueous gel as electrolyte for application in electrochromic devices based in bismuth electrodeposition. *J. Electrochem. Soc.* **150**, E578–E582.
- Kondo, K., Kouta, H., Yokoi, M., Okamoto, N., Saito, T., and Hayashi, T. (2014). Cuprous ion as an accelerant of copper damascene electrodeposition. *ECS Trans.* **58**, 89–96.
- Schmitt, K.G., Schmidt, R., von-Horsten, H.F., Vazhenin, G., and Gewirth, A.A. (2015). 3-Mercapto-1-propanesulfonate for Cu electrodeposition studied by in situ shell-isolated nanoparticle-enhanced Raman spectroscopy, density functional theory calculations, and cyclic voltammetry. *J. Phys. Chem. C* **119**, 23452–23462.
- Tobias, C.W. (1962). *Advances in Electrochemistry and Electrochemical Engineering, Vol. 2* (John Wiley).
- Gamburg, Y.D., and Zangari, G. (2011). *Theory and Practice of Metal Electrodeposition* (Springer).
- Qaimkhani, M.I., Siddiqui, R.A., Rauf, M., and Parveen, S. (2008). A new method for the preparation of copper oxychloride (a fungicide). *J. Chem. Soc. Pak.* **30**, 361–364.
- Beccaria, A.M., Mor, E.D., Bruno, G., and Poggi, G. (1982). Corrosion of lead in sea water. *Br. Corros. J.* **17**, 87–91.
- Bohren, C.F., and Huffman, D.R. (1983). *Absorption and Scattering of Light by Small Particles* (John Wiley).
- Granqvist, C.G. (2014). Electrochromics for smart windows: oxide-based thin films and devices. *Thin Solid Films* **564**, 1–38.
- Thakur, V.K., Ding, G., Ma, J., Lee, S.P., and Lu, X. (2012). Hybrid materials and polymer electrolytes for electrochromic device applications. *Adv. Mater.* **24**, 4071–4096.